Contents lists available at GrowingScience

Engineering Solid Mechanics

homepage: www.GrowingScience.com/esm

The microstructure and mechanical behavior of modern high temperature alloys

A.T. Samaei[a*], M.M. Mirsayar[b] and M.R.M. Aliha[c]

[a]*School of Engineering, University of California Merced, Merced, California 95343, USA*
[b]*Zachry Department of Civil Engineering, Texas A&M University, College Station, TX 77843-3136, USA*
[c]*Welding and Joining Research Center, School of Industrial Engineering, Iran University of Science and Technology, Narmak, 16846-13114 Tehran, Iran*

A R T I C L E I N F O	A B S T R A C T
	Over the past decades, high entropy alloys (HEAs) have attracted continuously increasing research efforts because of their technological promise for structural applications and their scientific interest as a multi-component alloy exhibiting an overall random solid solution structure with high mixing entropy at high temperature. In this summary, we briefly review the recent studies focused on the structure and mechanical behavior of HEAs, covering the important issues from phase stability to elastic modulus, mechanical strength, hardness and fatigue resistance. Finally, we highlight a few key findings recently reported for HEAs and discuss the outstanding issues yet to be resolved.

1. Introduction

The notion of 'High Entropy Alloy' (HEA) was proposed by Yeh and co-workers (2004a). Since then, a continuously increasing research interest has been simulated in the field of materials science and engineering because of the promise that, through the new routes of HEA design, materials scientists may obtain new alloys with novel properties which cannot be achieve otherwise in conventional alloys. Today, may HEAs become attractive for future structural applications, particularly at high temperature, because of their unique combinations of physical and mechanical properties (Yeh et al., 2004a; Chen et al., 2005; Tong et al., 2005; Huang et al., 2007; Wu et al., 2006; Chen et al., 2006; Zhou et al., 2007a). According to the original definition (Yeh et al., 2004a), HEAs are multi-component alloys in which the atomic fraction for each of their elements is nearly equal. This notion is rooted into the concept of an 'ideal' random solute solution, which yields the following configurational entropy of mixing ΔS_{conf}:

$$\Delta S_{conf} = -k \ln \omega = -R\left(\frac{1}{n} \ln \frac{1}{n} + \frac{1}{n} \ln \frac{1}{n} + \cdots \frac{1}{n} \ln \frac{1}{n}\right) = -R \ln \frac{1}{n} = R \ln n, \qquad (1)$$

where k, ω, and R are Boltzmann's constant, the number of ways of mixing, and the gas constant: 8.314 J/K mole, respectively. According to Eq. (1), ΔS_{conf} reaches its maximum when the alloy has an equi-atomic ratio. This explains why equal atomic fraction is preferred in the alloy design for HEAs. In general, Eq. (1) may hold for alloy systems above their melting point. If one further assumes that the same amount of configurational entropy of mixing still remains after solidification, HEAs, the alloy system with equal atomic fractions, thus arise, which are excepted to possess an intrinsic structural disordeness (or entropy) much greater than conventional alloys with one or two base elements.

Indeed, Cantor et al. (2004) might be the first one discovering the effect of high mixing entropy. Contrary to the common notion that intermetallics would be formed by mixing together different metallic elements with negative enthalpy of mixing, Cantor et al. (2004) found a single-phase solute solution structure in the FeCrMnCoNi alloy system without any obvious intermetallics phase. Later on, this behavior of forming solid solution rather than intermetallics in a multi-component alloy was attributed to the high mixing entropy effect by Yeh et al. (2004a). According to the literature (Yeh et al., 2004b; Yeh, 2013), HEAs would possess the following distinctive structural/ thermodynamic attributes as compared to conventional alloys: high mixing entropy, sluggish diffusion, lattice distortion, and 'cocktail' effects, out of which the high mixing entropy is expected to play the essential role in the alloy design and mechanical properties of HEAs.

Despite the fact that the alloy discovered by Cantor et al. (2004) is single-phased, most of the HEAs currently studied are of a multi-phased solid solution structure. Crystallographically, the typical atomic structure in HEAs include face centered cubic (FCC) and/or body centered cubic (BCC) crystal structure(s), with or without nano-precipitates (Yeh et al., 2004a; Tong et al., 2005). The complexity in the atomic structure of HEAs as accompanied by heavy solid solution strengthening, binding enhancement and fine-grain strengthening, can lead to superior mechanical properties at high temperatures, such as relatively high hardness (Huang et al., 2007; Lin et al., 2011)and mechanical strengths (Zhou et al., 2007a; Yang et al., 2012), good thermal stability (Sriharitha et al., 2014)and work hardenability (Varalakshmi et al., 2008), excellent anticorrosive properties (Chou et al., 2010a, b)and wear resistance (Wang et al., 2013, 2011), and unique magnetic properties (Tariq et al., 2013; Liu et al., 2012). Such a combination of impressive mechanical properties renders HEAs one of the most promising candidate structural materials for future engineering, and industrial applications, such as sport goods, nuclear technology, aerospace engineering, superconductorand hydrogen storage (2014; Otto et al., 2013a; Zhang et al., 2013; Tsai et al., 2013a; Sheng et al., 2013; Tsai et al., 2013b; Ng et al., 2012; Zhuang et al., 2012; Shun et al., 2012b; Hemphill et al., 2012; Zhang et al., 2012a; Senkov & Woodward, 2011a; Hsu et al., 2011).

In practice, HEAs can be synthesized by various experimental methods, including mechanical alloying, vacuum arc melting, sputtering and splat quenching (Sriharitha et al., 2014; Sheng et al., 2013; Qiu & Liu, 2013; Zhang et al., 2012b). Casting route have been widely used for HEAs preparation among the aforementioned processes, and it usually produced typically dendrite structure with some segregation in dendrite and interdendrite regions (Chen et al., 2006; Yeh et al. 2004a; Tong et al., 2005). On the other hand, it is reported that there will be formed a meta-stable phases during sputtering or splat quenching, however it may become stable after annealing at high temperature (Yeh et al., 2004a).Some studies have shown that mechanical alloying lead to a HE alloy with more homogenous and stable nano-crystalline microstructures (Chen et al., 2009 a,b). In spite of the intense research endeavors, however, a few fundamental issues still remain unresolved, such as phase stability, atomic-scale deformation mechanisms, and the structure-property relation. At the present, these constitute the central theme of research in the area of HEAs. In this article, we would like to summarize the recent research efforts dedicated to resolve these outstanding issues.

2. Microstructure of High Entropy Alloys

2.1. Thermodynamic and Phase Stability

In the case of HEAs, there has been presented a very few theories based on the thermodynamic properties for predicting the microstructure formation and phases (Zhang et al., 2008; Hsieh et al., 2009; Wang et al., 2009b; Lin & Tsai, 2010a).The morphological stability and the nature and dynamic behavior of the phases in the formation of HEAs are the essential challenges to understand their microstructure and predict their physical and mechanical properties for designing an optimized alloy system for special application. The maximum number of equilibrium phases at constant pressure can be predicted based on the Gibbs phase rule by using the relation

$$F = C - P + 1 \;,\tag{2}$$

where F, C, and P are degree of freedom, number of components, and number of phase, respectively. However, the number of phases appeared in multi-element HEA systems is not in accordance with the aforementioned rule, and it usually is far less than the maximum prediction due to the high mixing entropy effect, which caused to restrain the formation of intermetallic compounds (Yeh et al., 2004b). For example, the number of components was six in the AlCoCrCuFeNi HEA system, but the actual number phase reported by Tung et al. (2007) was only three (included FCC, BCC,HCP and ordered BCC) which is far less than the highest value of phases 7. A few studies have thermodynamically investigated the phase formation rule for illustration the decreasing of Gibbs energy ($\Delta G_{mix} = \Delta H_{mix} - T\Delta S_{mix}$), where ΔG_{mix}, ΔH_{mix}, ΔS_{mix}, and T are the Gibbs energy, the enthalpy of mixing, the entropy of mixing, and the absolute temperature, respectively, of the solid solution at elevated temperatures led to the formation of simple solid solutions against intermetallic compounds due to forming random solid solution easily and more stable than the other phases in HEA systems. Based on the completely random mixing, the entropy of mixing of multi-component alloy systems with n element is

$$\Delta S_{mix} = -R \sum_{i=1}^{n} c_i \ln c_i\tag{3}$$

where R and c_i are the gas constant and the mole percentage of the ith component, and also $\sum_{i=1}^{n} c_i = 1$. Due to this mixing entropy which becomes a maximum for equi-atomic alloys like AlCoCrFeNiTi, HEA systems have much higher mixing entropies than the conventional multicomponent alloys (Zhou et al., 2007b).In addition, the slow diffusion kinetics accompanies the formation of simple solid solutions because of the difficult cooperation among the migrants of various elements, and the activation energies related to the number of composing elements in the matrix of HEAs correspondingly are higher than the conventional multicomponent alloys (Tsai et al. 2013b).
Recently, some investigations have conducted to determine the rules governing the phase stability in high entropy alloys regarding relevancy to the formation of solid solutions, intermetallic, and amorphous phases based on a statistical analysis of the constituent elements in a large database of these alloys. Guo et al. (2013) have highlighted two types of factors controlling the aforementioned phase selection: 1) topological (mainly the atomic size), for example, the atomic size difference for solid solution phases is small against amorphous phases, 2) chemical (the electronegativity, electron concentration or the mixing enthalpy), as instance, the mixing entropy and mixing enthalpy of amorphous phases are more negative and smaller than those of the solid solution phases. For the multicomponent alloys, Zhang et al. (2012c) firstly defined three parameters, which are the atomic size difference (δ) which plays an essential role in the glass transition of hard-sphere colloidal systems (Guo et al., 2013), the mixing enthalpy (ΔH_{mix}), and the mixing entropy (ΔS_{mix}), to characterize the collective behavior of constituent elements as

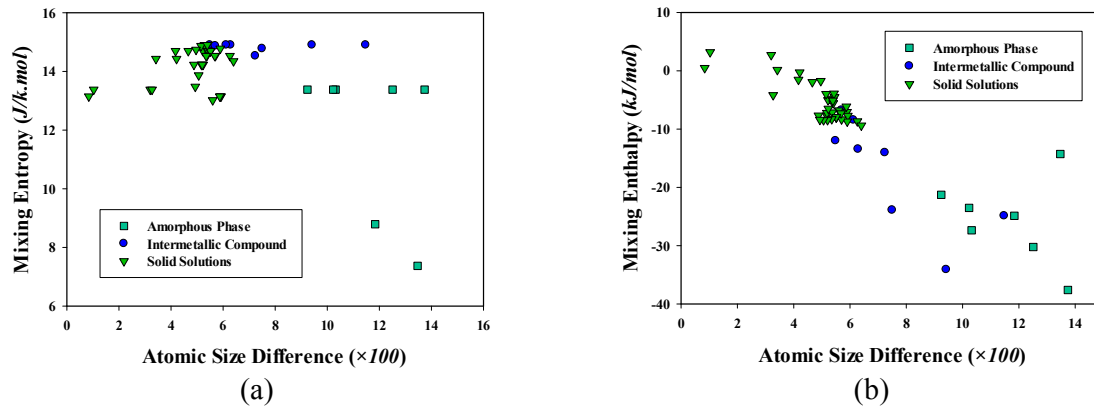$$\delta = \sqrt{\sum_{i=1}^{n} c_i(1 - r_i/\bar{r})^2} \tag{4}$$

where $\bar{r} = \sum_{i=1}^{n} c_i r_i$, r_i is atomic radius of the ith element. The mixing enthalpy is given as $\Delta H_{mix} = \sum_{i=1,i \neq j}^{n} \Omega_{ij} c_i c_j$, where $\Omega_{ij} = 4\Delta_{mix}^{AB}$, Δ_{mix}^{AB} is the mixing enthalpy of binary liquid AB alloys (Takeuchi & Inoue, 2000). Δ_{mix}^{AB}, assuming a random solid solution of atom A in B, is obtained by using the Miedema's model (Egmai & Waseda, 1984) considered only the chemical contribution, and it implies that the electronegativity effect is included in this model.

For a series of equiatomic or nearly equiatomic alloys, the mixing entropy(ΔS_{mix}), the mixing enthalpy(ΔH_{mix}), and atomic radius difference (δ) were calculated based on above equations and listed in Table 1.These alloys were prepared by the arc melting, injection melting, copper mold casting, and melt spinning, and the phases mentioned in Table 1 are mostly referring to the as-cast state, which most of the solid solution phases in HEAs are quite stable near to the equilibrium state (Wen et al., 2009; Lin et al., 2010 b, c). However, the cooling rates, the kinetic nature of transition, and other thermodynamic parameters are determinant for the formation amorphous phases. It proposed that the fundamental thermodynamic parameters and properties of the elements in preparation of alloys do make a difference on forming the phases such as solid solution, amorphous, and intermetallic phases, for example, any alloy can form amorphous phases from liquid state by using a sufficient cooling rate (Cohen &Turnbull, 1961).On the other hand, there are some investigations shown some equiatomic or near equiatomic alloys cannot form the amorphous phases even by aforementioned conditions (Cantor et al., 1976).The atomic size difference of SrCaYbMgZn (AM), ErTbDyNiAl (AM), ZrHfTiCuNi (AM), ZrHfTiCuFe (AM),WNbMoTa (SS), WNbMoTaV (SS), FeCoNiCrCu (SS), FeCoNiCrCuAl$_{0.3}$ (SS), AlCoCrCuFe$_{0.5}$Ni (SS), CoCrFeNiTi (IM), NbCrFeMnCoNi (IM)(Cantor et al. 2004), andTi$_2$CrCuFeCoNi (IM)was obtained to be 15.25, 13.74, 10.32, 10.42, 2.31, 3.15, 1.03, 3.42, 5.4, 6.68, 5.49, and 7.24, respectively, which AM, SS, and IM denote to amorphous, solid solution, and intermetallic phases, respectively (Gao et al., 2011; Ma et al., 2002; Senkov et al., 2010; Tang et al., 2007). It implies that severe lattice distortion may lead to amorphous tendency due to large atomic size difference (Tsai et al. (2013a)). It is found that the phases tends to form in the domain defined as follows: 1- solid solution (SS) phases: $0 \leq \delta \leq 8.5$, $-22 \leq \Delta H_{mix} \leq 7$ kJ/mol, and $11 \leq \Delta S_{mix} \leq 19.5$ kJ/mol, 2- the amorphous (AM) phases: $4.5 \leq \delta \leq 18.5$, $-50 \leq \Delta H_{mix} \leq -8$ kJ/mol, and $7 \leq \Delta S_{mix} \leq 17.5$ kJ/mol, and 3- intermetallic (IM) phases: $4 \leq \delta \leq 11.5$, $-35 \leq \Delta H_{mix} \leq -4$ kJ/mol, and $13 \leq \Delta S_{mix} \leq 17.5$ kJ/mol.

Fig. 1 shows the presented data in Table1 to illustrate the three main parameters governing the phase stability such as mixing entropies (ΔS_{mix}), mixing enthalpy (ΔH_{mix}), andthe atomic radius difference (δ)indicating the collective behavior of the constituent elements for all three mentioned phases and also presenting the phase formation regions as defined above. From Fig.1, it is found that the above phases form in approximately separate regions from each other: 1- the solid solution (SS) phases: high mixing entropy, mostly positive mixing enthalpy, and small atomic size difference, 2- the intermetallic (IM) phases: moderately high mixing entropy, negative mixing enthalpy, and moderately high atomic size difference, 3- the amorphous (AM) phases: smaller mixing entropy, more negative mixing enthalpy, and high atomic size difference. Therefore, the formation of these three phases can be determined by noting to the mixing entropies and mixing enthalpy in terms of the atomic size difference of alloys. For example, when the mixing entropy is high and the mixing enthalpy is correspondingly very negative, the phase is suggested amorphous one based on the statistical analyses indicated in the Table 1 and Fig.1.For the phase selection or prediction in alloys especially high entropy alloys, it has been shown that the two alloy composition physical parameters, atomic size difference (δ) and mixing enthalpy (ΔH_{mix}) are necessary but not sufficient conditions by preparation some new alloys using the melt spinning method (Guo et al., 2013).

Table 1. Calculated parameters, atomic size difference (δ), mixing enthalpy (ΔH), mixing entropies (ΔS), and phases (AM: Amorphous, SS: Solid Solution, and IM: Intermetallic) used in Fig. 2 (a) and (b).

Material	$\delta (\times 100)$	ΔH	ΔS	Phase	Reference
ErTbDyNiAl	13.74	-37.6	13.38	AM	Gao et al. (2011)
ZrHfTiCuNi	10.32	-27.36	13.38	AM	Ma et al. (2002)
ZrHfTiCuCo	10.23	-23.52	13.38	AM	Ma et al. (2002)
ZrTiNiCuBe	12.51	-30.24	13.38	AM	Takeuchi and Inoue (2001)
$Cu_{46}Zr_{42}Al_7Y_5$	11.84	-24.88	8.79	AM	Li et al. (2007)
$Ca_{65}Mg_{15}Zn_{20}$	13.47	-14.26	7.37	AM	Li et al. (2007)
FeCoNiCrCu	1.03	3.2	13.38	SS	Tong et al. (2005)
$FeCoNiCrCuAl_{0.3}$	3.42	0.16	14.43	SS	Tong et al. (2005)
$FeCoNiCrCuAl_{0.5}$	4.17	-1.52	14.7	SS	Tong et al. (2005)
$FeCoNiCrCuAl_{1.0}$	5.28	-4.78	14.9	SS	Tong et al. (2005)
$FeCoNiCrCuAl_{1.5}$	5.89	-7.05	14.78	SS	Tong et al. (2005)
$FeCoNiCrCuAl_{2.0}$	6.26	-8.65	14.53	SS	Tong et al. (2005)
$FeCoNiCrCuAl_{2.3}$	6.4	-9.38	14.35	SS	Tong et al. (2005)
$AlCo_{0.5}CrCuFeNi$	5.45	-4.5	14.7	SS	Tung et al. (2007)
$AlCoCr_{0.5}CuFeNi$	5.22	-5.02	14.7	SS	Tung et al. (2007)
$AlCoCrCu_{0.5}FeNi$	5.51	-7.93	14.7	SS	Tung et al. (2007)
$AlCoCrCuFe_{0.5}Ni$	5.4	-5.55	14.7	SS	Tung et al. (2007)
$AlCoCrCuFeNi_{0.5}$	5.43	-3.9	14.7	SS	Tung et al. (2007)
$CoCrCu_{0.5}FeNi$	0.84	0.49	13.15	SS	Tung et al. (2007)
$AlCoCrCu_{0.5}FeNi$	5.51	-7.93	14.7	SS	Ke et al. (2006)
$AlCrCu_{0.5}FeNi$	5.92	-7.7	13.15	SS	Ke et al. (2006)
$AlCoCrCu_{0.5}FeNi$	5.51	-7.93	14.7	SS	Ke et al. (2006)
$AlCo_2CrCu_{0.5}FeNi$	5.17	-7.67	14.23	SS	Ke et al. (2006)
$AlCo_3CrCu_{0.5}FeNi$	4.88	-7.67	14.23	SS	Ke et al. (2006)
$AlCoCu_{0.5}FeNi$	5.9	-8.69	13.15	SS	Ke et al. (2006)
$AlCoCrCu_{0.5}FeNi$	5.51	-7.93	14.7	SS	Ke et al. (2006)
$AlCoCr_2Cu_{0.5}FeNi$	5.18	-7.2	14.23	SS	Ke et al. (2006)
$AlCoCrCu_{0.5}Fe_{0.5}Ni$	5.66	-8.92	14.53	SS	Ke et al. (2006)
$AlCoCrCu_{0.5}FeNi$	5.51	-7.93	14.7	SS	Ke et al. (2006)
$AlCoCrCu_{0.5}Fe_{1.5}Ni$	5.37	-7.14	14.53	SS	Ke et al. (2006)
$AlCoCrCu_{0.5}Fe_2Ni$	5.23	-6.49	14.23	SS	Ke et al. (2006)
$AlCoCrCu_{0.5}Fe$	5.87	-6.12	13.15	SS	Ke et al. (2006)
$AlCoCrCu_{0.5}FeNi_{0.5}$	5.68	-7.28	14.53	SS	Ke et al. (2006)
$AlCoCrCu_{0.5}FeNi$	5.51	-7.93	14.7	SS	Ke et al. (2006)
$AlCoCrCu_{0.5}FeNi_{1.5}$	5.35	-8.28	14.53	SS	Ke et al. (2006)
$AlCoCrCu_{0.5}FeNi_2$	5.2	-8.43	14.23	SS	Ke et al. (2006)
$AlCoCrCu_{0.5}FeNi_{2.5}$	5.06	-8.45	13.87	SS	Ke et al. (2006)
$AlCoCrCu_{0.5}FeNi_3$	4.93	-8.39	13.48	SS	Ke et al. (2006)
CrCuFeMnNi	3.2	2.72	13.38	SS	Chen et al. (2006)
CoCrFeMnNi	3.27	-4.16	13.38	SS	Cantor et al. (2004)
$Al_{0.3}CrCuFeMnNi$	4.21	-0.27	14.43	SS	Chen et al. (2006)
$Al_{0.5}CrCuFeMnNi$	4.66	-1.92	14.7	SS	Chen et al. (2006)
$Al_{0.8}CrCuFeMnNi$	5.15	-3.97	14.87	SS	Chen et al. (2006)
AlCrFeMnNi	5.39	-5.11	14.9	SS	Chen et al. (2006)
$Al_{0.8}CrCu_{1.5}FeMnNi$	4.96	-1.74	14.74	SS	Chen et al. (2006)
NbCrFeMnCoNi	5.49	-12	14.9	IM	Cantor et al. (2004)
TiCrFeMnCoNi	6.29	-13.44	14.9	IM	Cantor et al. (2004)
$Ti_2CrCuFeCoNi$	7.24	-14.04	14.53	IM	Zhang et al. (2008)
ZrTiVCuNiBe	11.48	-24.89	14.9	IM	Zhang et al. (2008)
$CoCrCuFeNiTi_{0.8}$	5.7	-6.75	14.87	IM	Wang et al. (2007)
$CoCrCuFeNiTi_{1.0}$	6.12	-8.44	14.9	IM	Wang et al. (2007)
$AlCoCrFeNiTi_{1.5}$	7.5	-23.91	14.78	IM	Zhou et al. (2007a)

(a)   (b)

Fig. 1. The phase selection in high entropy alloys based on the calculated parameters in Table 1, (a) mixing entropy vs. atomic size difference, (b) mixing enthalpy vs. atomic size difference.

Due to possessing the larger mixing entropies, simple solid solutions with more principal elements tend to be more stable than the intermetallic compounds in high entropy alloys. Therefore, the decomposition into multiple phases during casting in HEAs will be prevented because the high mixing entropy stabilizes solid solution phases. Based on the aforementioned formula of Gibbs energy and Boltzmann's hypothesis between the entropy and the complexity of the alloy system (Swalin et al., 1991), Zhou et al. (2007a) have explained the effect of high mixing entropy indicative the formation of phases in HEAs such as decreasing the free energy caused to be more stable at elevated temperature (Ranganathan, 2003), relaxing the constraints led to form substitution solid solutions and balancing the lattice strain give rise to make solid solution more stable than intermetallic, especially at high temperature. Although most of the HEAs described in the literature consist of multiple phases and/or intermetallic compounds, there are some studies reported a single phase solid solution such as FCC or BCC and presented no tendency to form complex or multiple phases due to increasing the number of elements. In addition, some researchers presented a combination of solid solutions and intermetallic phases in the formation of HEAs and evaluated effects of these combinations on the mechanical properties of these alloy systems. For example, Wang et al. (2009 b) found the great influences of the formation of multiple phases included solid solution and intermetallic phases on the mechanical and magnetic properties ofAlCrFeCoNiCu HE alloy. Yeh et al. (2004a) mentioned several factors for the formation of phases in HEAs, and one of those factors is large lattice distortions led to lower diffusion rates of atoms and then to reduce the nucleation and growth rates of crystallites which conclude some of HEA systems have nano-crystallites and even amorphous structures. Therefore, due to the concepts of both high mixing entropies and large lattice distortions for HEA systems, these alloys exhibit a new route of metallic materials with excellent thermal stabilities and diffusion resistance.

The formation of microstructure and equilibrium state are an outcome of stability competition among the phases, which it can be provided by using the phase diagrams as a function of temperature and composition in alloy systems. However, the determination of phase diagrams is much more challenging for multicomponent systems and high entropy alloys than the binary and simple ternary systems because of the wide ranges of composition and temperature (Zhang et al., 2012b). CALPHAD approach, a phenomenological approach that both measured phase equilibrium data and thermodynamic properties for a system will be separately transmuted to a unique thermodynamic description, has been extensively used for the investigation of phase equilibria of multicomponent systems and ultimately predict the thermodynamic properties of them in recent years (Kaufman & Bernstein, 1970).There are a few reports on calculating the phase diagram for high entropy alloys (Zhang et al., 2012a; Kaufman & Bernstein, 1970; Manzoni et al., 2013a). For example, Zhang et al. (2012a) used the aforementioned approach to predict the FCC/BCC phase transition of both as-cast and homogenized Al_xCoCrFeNi high entropy alloys and compared with the available literature data. Due to the essential importance of the thermodynamic calculations on the understanding of the phase stability in HEA systems, it is expected that phase diagram of these kind of metallic materials will be made for the future applications. There exist some studies that reported the non-equilibrium processing methods such as rapid solidification and mechanical alloying to obtain better physical and chemical properties like avoiding component segregation, improving solubility, producing nanocrystalline, stable microstructures with better homogeneity and etc. in the HEA systems (Praveen et al., 2013; Mridha et al., 2013).

2.2 Microstructure

Most of the research efforts are focused on the controlling the morphology and distribution of the beneficial minority phases and avoiding micro-segregation related to the formation of detrimental minority phases such as sigma phases in Cr- and Mo-rich in Ni-base for intermetallic compounds (Perricone et al., 2003) and also Fe- and Mn-rich in Al-base alloys (Khalifa et al., 2003) caused serious problems during thermo-mechanical treatment. For example, the ternary or higher order intermetallic compounds, which form unexpectedly in multi-component alloys at elevated operating temperatures,

include complex crystal structures that indicate a reduction in mechanical properties and microstructure stability. Recently, the process of microstructure formation during solid solution and solidification for HEAs with specially five components caused to stabilize solid solution like phases with simple crystal structures included FCC and/or BCC crystal structures rather than forming the complex intermetallic phases has been considerably investigated (Manzoni et al., 2013b; Koundinya et al., 2013). In spite of the complex composition of HEAs, their microstructure is simple which motivate researchers to explore, discover, and develop this new class of metallic materials possessing the high strength, light weight, and high temperature alloys characteristics for the future structural applications. There are a few studies for investigating the relation between the mechanical properties such as precipitation hardening and the morphology, phase and structure of precipitates in high entropy alloys (Tsai et al., (2013 d)). For example, Tsai et al. (2013 d) have reported the morphology, crystal structure and composition of the precipitates in a high entropy alloy. Some representative examples of microstructure of high entropy alloys formed during solidification are shown in Fig.2. Fig. 2(a) and Fig. 2(b) show the microstructure of the as-cast $Al_{0.5}CoCrCuFeNi$ HEA possessed both the dendritic (I) and interdendritic (II) regions (Ng et al. (2012) and the $Al_{0.9}CrCuFeNi_2$ HEA included the aforementioned regions (Guo et al., 2013), respectively. Fig. 2(c) indicates the microstructure of $Al_{2.0}CrCuFeNi_2$ composed of densely distributed colonies, with sunflower and petal-like morphologies (Guo et al., 2013). Fig. 2(d), 2(e), and 2(f) show the SEM microstructures of as-cast and annealed $Al_{0.5}CoCrFeCuNi$ alloys, and typical as-cast dendrite and interdendrite structures are observed in all cases, and the interdendrite contains large amounts of nanoparticles and nanorods (Sheng et al., 2013).
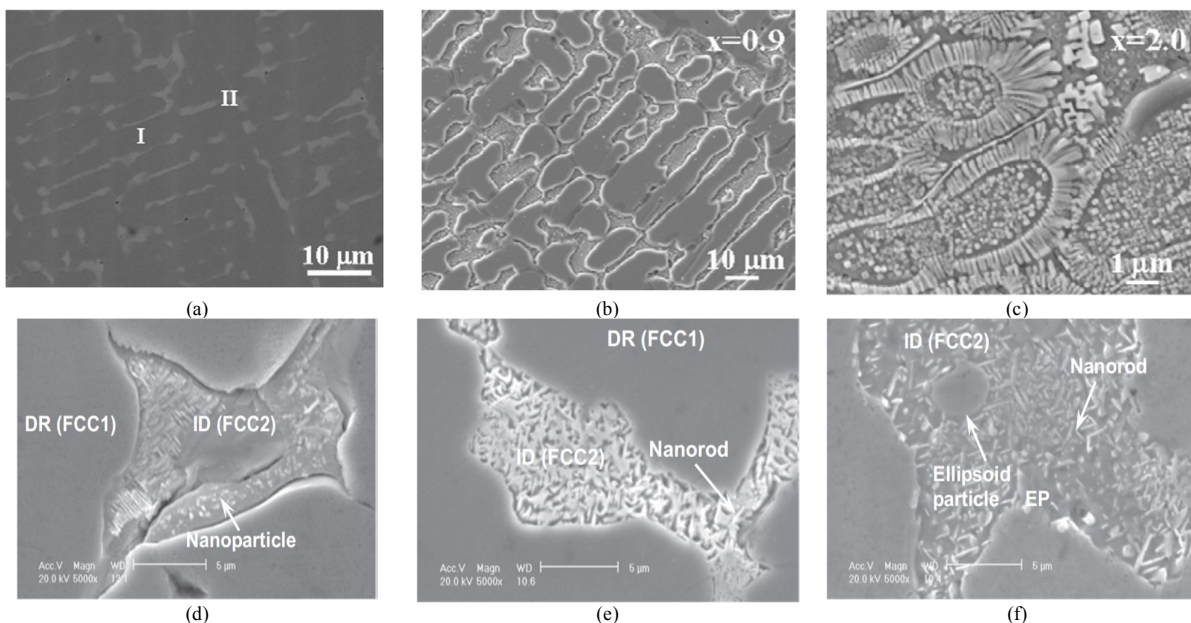

Fig. 2. Microstructures for the different high entropy alloys: (a) the as-cast $Al_{0.5}CoCrCuFeNi$ HEA (Ng et al. 2012), (b) the as-cast $Al_{0.9}CrCuFeNi_2$ HEA(Guo et al. 2013), (c) the as-cast $Al_{0.2}CrCuFeNi_2$ HEA (Guo et al. 2013), (d) the as-cast $Al_{0.5}CoCrFeCuNi$ HEA (Sheng et al. 2013),(e) the annealed $Al_{0.5}CoCrFeCuNi$ alloy at 600 ºC (Sheng et al. 2013),(f) the annealed $Al_{0.5}CoCrFeCuNi$ alloy at 800 ºC (Sheng et al. 2013).

Most of the studies on the HEAs indicate the same morphology like dendritic, interdendritic, and eutectic features for solidified microstructure of these alloys prepared by various techniques such as casting or arc melting (Yeh et al., 2004a; Tsai et al., 2013c; Zhang et al., 2012a; Hsieh et al., 2009; Zhang et al., 2011; Yu et al., 2013), and almost all of them state that the interdendritic region is much smaller than the dendritic domain shown the discontinuity in the alloy morphology. The difference between the compositions of the dendritic and interdendritic regions can be formed by non-equilibrium solidification, which this effect is known as interdendritic segregation, and dendritic and interdendritic

regions preferentially consist of the elements with high melting points and low melting points, respectively (Lin & Cho, 2009).In addition, the various produced microstructure features such as plate-like (Tariq et al., 2013), spherical (Tsai et al., 2013d), seed-like (Guo et al.,2013), disk floret (Guo et al.,2013), ribbon-like (Guo et al., 2013), rod-like (Guo et al., 2013), needle-like (Tariq et al., 2013)and sunflower-like (Guo et al., 2013) in both dendritic and interdendritic regions of HEAs have been reported (Tariq et al., 2013; Guo et al., 2013), and several reasons have been mentioned for those formations such as occurrence of spinodal decomposition (Inoue, 2000), volume percentage of phases (Guo et al., 2013), and the rate of growth in a phase (Guo et al., 2013), etc. Several investigations have shown that the dendritic regions are enriched with heavier elements than the interdendritic regions by using the decomposition of these alloys (Otto et al., 2013b). Since eutectic alloys indicate better performance and behavior in high temperature applications, some investigations attempted to control the solidification process for minimizing the interdendritic formation and making the fine microstructure. In addition, some investigations have stated that the multi-element σ phase due to the sluggish diffusion of atoms in the matrix could be helpful in morphology of HEAs and also could improve the mechanical properties such as hardness and toughness of them (Yeh et al., 2004a).

3. Mechanical Properties of HEAs

3.1. Elastic Modulus

With the development of more and more high entropy alloy systems, there exist a strong interest to recognize the mechanical properties such as elastic properties, yield strength, hardness, ductility, fatigue properties, etc. for the future applications of these new class of metallic materials. There are very few data and experimental phenomena on the elastic properties of the HEAs (Zhang et al., 2009; Singh et al., 2011), and the challenge is to explore the correlations among the elastic moduli and thermodynamic, kinetic, compositions and apply such understanding to develop new HEA systems with desirable properties. Table 2 lists the available elastic modulus of HEA systems accompanied with their phases and microstructural information. From Table 2, it is obvious that HEAs have considerably different microstructure and mechanical properties such as elastic modulus due to their different phase formations.

Zhang et al. (2009) investigated the effect of addition of Al on the compressive strength and elastic modulus of $CoCrFeNiTiAl_x$ HEA system, and they found that the elastic moduli of this alloy increased as the Al contents increasing from $x = 0$ to 2.0. For example, the elastic modulus for Al_0 and $Al_{1.0}$ reach as high as 134.6 GPa and 147.6 GPa, respectively. They stated that this phenomenon can be related to the different crystal structure such as BCC and FCC because of adding Al, and BCC crystal structure has lower atomic packing efficiency and lattice strain than FCC structure (Zhang et al., 2009). Singh et al. (2011) investigated the hardness and indentation elastic moduli of both the splat-quenched and as-cast HEAs, and they found that the hardness of them is almost equal, however, the indentation elastic modulus of as-cast HEAs is considerably higher than that of the splat-quenched HEAs. The elastic moduli can be considered for predicting new HEA systems with controlled mechanical properties and assist in selecting the component of alloys for improving the microstructure and properties led to a new HEA design. The ability for making HEA systems with specific elastic properties will open new opportunities for fabrication of instruments and manufacturing of structures in nuclear technology, aerospace structures, racket frame, tools production, superconductor, hydrogen storage materials for mobile, golf striking face plate and etc.

Material	Phase	Morphology	structure	Elastic Modulus (GPa)	Yield Stress (MPa)	Hardness (Hv)	Preparation Method	Ref.
CuCoNiCrAl$_{1.5}$Fe	SS	DR+ID+B2+A2	FCC+BCC	-	-	500	Arc melting	Yeh et. al.(2004a)
CuCoNiCrAl$_{2.0}$Fe	SS	DR+ID+B2+A2	FCC+BCC	-	1600	580	Arc melting	Yeh et. al.(2004a)
CuCoNiCrAl$_{2.8}$Fe	SS	DR+ID+B2+A2	BCC	-	-	655	Arc melting	Yeh et. al.(2004a)
AlCoCrCuNi	SS	DR+ID+B2	FCC+BCC	-	-	419±6	Arc melting+Casting	Hsu et al. (2007)
AlCoCrCuFeNi	SS	DR+ID+B2	FCC+BCC	-	-	416±19	Arc melting+Casting	Hsu et al. (2007)
AlAuCoCrCuNi	SS	DR+ID+B2	FCC+ AuCu	-	-	276±8	Arc melting+Casting	Hsu et al. (2007)
Golden layer of	SS	DR+ID+B2	Ag + FCC	-	-	104±3	Arc melting+Casting	Hsu et al. (2007)
Silver layer of	SS	DR+ID+B2	BCC+Ag + FCC	-	-	451±9	Arc melting+Casting	Hsu et al. (2007)
AlCoCrCuFeNi	SS	DR+ID	FCC+BCC	-	-	420	Arc melting+Casting	Tung et al. (2007)
Al$_{0.5}$CoCrCuFeNi	SS	DR+ID	FCC	-	-	208	Arc melting+Casting	Tung et al. (2007)
AlCo$_{0.5}$CrCuFeNi	SS	DR+ID	FCC+BCC	-	-	473	Arc melting+Casting	Tung et al. (2007)
AlCoCr$_{0.5}$CuFeNi	SS	DR+ID	FCC+BCC	-	-	376	Arc melting+Casting	Tung et al. (2007)
AlCoCrCu$_{0.5}$FeNi	SS	DR+ID	BCC	-	-	458	Arc melting+Casting	Tung et al. (2007)
AlCoCrCuFe$_{0.5}$Ni	SS	DR+ID	FCC+BCC	-	-	418	Arc melting+Casting	Tung et al. (2007)
AlCoCrCuFeNi$_{0.5}$	SS	DR+ID	FCC+BCC	-	-	423	Arc melting+Casting	Tung et al. (2007)
TiVCrMnFeCoNiCu	SS+A	DR+ID	FCC+BCC+σ	74.247	1312	-	Arc melting	Zhou et al. (2007a)
Al$_{11.1}$(TiVCrMnFeCo	SS	DR+ID	FCC+BCC+σ	164.087	1862	-	Arc melting	Zhou et al. (2007b)
Al$_{20}$(TiVCrMnFeCo	SS	DR+ID	FCC+BCC+σ	190.086	1465	-	Arc melting	Zhou et al. (2007b)
AlCrFeCoNiCu	SS	DR+ID+EC	FCC+BCC	-	1303	-	Vacuum arc melting	Li et al. (2008)
AlCrFeCoNiCuMn	SS	DR+ID+EC	FCC+BCC	-	1005	-	Vacuum arc melting	Li et al. (2008)
AlCrFeCoNiCuTi	SS	DR+ID+EC	FCC+BCC	-	1234	-	Vacuum arc melting	Li et al. (2008)
AlCrFeCoNiCuV	SS	DR+ID+EC	FCC+BCC	-	1469	-	Vacuum arc melting	Li et al. (2008)
AlCrFeCoNi	SS	DR+ID	BCC	-	1250.96	-	Vacuum arc melting	Wang et al. (2008)
CrFeCoNiCuTi	SS	DR+ID	BCC	-	1272	-	Vacuum arc melting	Wang et al. (2008)
AlCrMnFeCoNiCuTi	SS	DR+ID	BCC	-	1862	-	Vacuum arc melting	Wang et al. (2008)
CrFeCoNiCuTi$_{0.5}$	SS	DR+ID	BCC	-	700	-	Vacuum arc melting	Wang et al. (2008)
CoCrFeNi	SS	DR+ID	FCC	-	-	116±3	Vacuum arc melting	Kao et al. (2009)
Al$_{0.5}$CoCrFeNi	SS	DR+ID	FCC+BCC	-	-	159±2	Vacuum arc melting	Kao et al. (2009)
Al$_{1.0}$CoCrFeNi	SS	DR+ID	FCC+BCC	-	-	484±26	Vacuum arc melting	Kao et al. (2009)
Al$_{2.0}$CoCrFeNi	SS	DR+ID	BCC	-	-	509±27	Vacuum arc melting	Kao et al. (2009)
FeNiCrCuCo	SS	DR+ID	FCC	-	-	286	Arc melting	Li et al. (2009)
FeNiCrCuMo	SS	DR+ID	FCC	-	-	263	Arc melting	Li et al. (2009)
FeNiCrCuAl	SS	DR+ID	FCC+BCC	-	-	342	Arc melting	Li et al. (2009)
FeNiCrCuMn	SS	DR+ID	FCC+BCC	-	-	296	Arc melting	Li et al. (2009)
FeNiCrCoAl	SS	DR+ID	BCC	-	-	395	Arc melting	Li et al. (2009)
Fe NiCrCoAl$_2$	SS	DR+ID	BCC	-	-	432	Arc melting	Li et al. (2009)
FeNiCrCoAl$_3$	SS	DR+ID	BCC	-	-	506	Arc melting	Li et al. (2009)
FeNiCrCuZr	SS+I	DR+ID	BCC+Compound	-	-	566	Arc melting	Li et al. (2009)
Al$_{0.5}$CoCrCuFeNi	SS+I	DR+ID	FCC+BCC	-	-	208±2	Arc melting	Tsai et al. (2009)
Ti$_{0.5}$CrFeCoNiCu	SS	DR+ID	FCC	92.73	1650	-	Arc melting	Wang et al. (2009a)
Ti$_{0.5}$CrFeCoNiAl$_{0.5}$C	SS	DR+ID	FCC+BCC	160.54	2389	-	Arc melting	Wang et al. (2009a)
Ti$_{0.5}$CrFeCoNiAl$_{0.75}$C	SS	DR+ID	FCC+BCC	164.14	2697	-	Arc melting	Wang et al. (2009a)
CoCrFeNiTiAl$_{0.5}$	SS	DR+ID	BCC+B2+Laves	106.8	1600	-	Vacuum arc melting	Zhang et al. (2009)
CoCrFeNiTiAl$_{1.0}$	SS	DR+ID	BCC+B2+Laves	147.6	2280	-	Vacuum arc melting	Zhang et al. (2009)
CoCrFeNiTiAl$_{2.0}$	SS	DR+ID	BCC	93.5	1030	-	Vacuum arc melting	Zhang et al. (2009)
Al$_{0.3}$CrFe$_{1.5}$MnNi$_{0.5}$	SS	DR+ID	FCC+BCC+B2	-	-	297±2	Arc melting & Casting	Chen et al. (2010)
Al$_{0.5}$CrFe$_{1.5}$MnNi$_{0.5}$	SS	DR+ID	FCC+BCC+B2	-	-	396±7	Arc melting & Casting	Chen et al. (2010)
AlCo$_{0.5}$CrFeMo$_{0.5}$Ni	SS	DR	BCC+σ	-	-	788	Arc melting	Hsu et al. (2010)
AlCo$_{2.0}$CrFeMo$_{0.5}$Ni	SS	DR	FCC+BCC+σ	-	-	596	Arc melting	Hsu et al. (2010)
Al3CoCrFeNi	SS	DR+ID	BCC+B2	-	-	740	Arc melting & Casting	Li et al. (2010)
CoCrFeNiCuAl	SS	DR+ID	FCC+BCC+B2	-	1820	515.5	Vacuum arc melting	Zhang et al. (2010)
AlCoCrFeNi	SS	LE	BCC	-	1051	-	Copper mold casting	Zhu et al. (2010a)
AlCoCrFeNiMo$_{0.2}$	SS	LE	BCC+α	-	2456	-	Copper mold casting	Zhu et al. (2010a)
AlCoCrFeNiMo$_{0.5}$	SS	LE	BCC+α	-	2757	-	Copper mold casting	Zhu et al. (2010a)
AlCoCrFeNi	SS	-	BCC	-	1110	-	Arc melting	Zhu et al. (2010b)
AlCoCrFeNiSi$_{0.4}$	SS	NC	BCC	-	1481	-	Arc melting	Zhu et al. (2010b)
AlCoCrFeNiSi$_{1.0}$	SS	NC	BCC+δ	-	2411	-	Arc melting	Zhu et al. (2010b)
Co$_{1.5}$CrFeNi$_{1.5}$Ti$_{0.5}$	SS	DR+ID	FCC+γ	-	-	509±11	Arc melting	Chuang et al. (2011)
Al$_{0.2}$Co$_{1.5}$CrFeNi$_{1.5}$Ti$_0$	SS	DR+ID	FCC+γ	-	-	487±5	Arc melting	Chuang et al. (2011)
Co$_{1.5}$CrFeNi$_{1.5}$Ti$_{1.0}$	SS	DR+ID	FCC+η	-	-	654±7	Arc melting	Chuang et al. (2011)
Al$_{0.2}$Co$_{1.5}$CrFeNi$_{1.5}$Ti$_1$	SS	DR+ID	FCC+η	-	-	717±13	Arc melting	Chuang et al. (2011)
AlCoFeMo$_{0.5}$Ni	SS	DR+ID	B2+σ	-	-	600	Arc melting	Hsu et al. (2011)
AlCoCr$_{1.0}$FeMo$_{0.5}$Ni	SS	DR+ID	B2+σ	-	-	730	Arc melting	Hsu et al. (2011)
AlCoCr$_{1.5}$FeMo$_{0.5}$Ni	SS	DR+ID	B2+σ	-	-	820	Arc melting	Hsu et al. (2011)
AlCoCr$_{2.0}$FeMo$_{0.5}$Ni	SS	DR+ID	B2+σ	-	-	870	Arc melting	Hsu et al. (2011)
Nb$_{25}$Mo$_{25}$Ta$_{25}$W$_{25}$	SS	DR+ID	BCC	220±20	1058	-	Vacuum arc melting	Senkov et al. (2011b)
V$_{20}$Nb$_{20}$Mo$_{20}$Ta$_{20}$W$_{20}$	SS	DR+ID	BCC	180±5	1246	-	Vacuum arc melting	Senkov et al. (2011b)
AlCoCrCuFeNi	SS	DR+ID	FCC+BCC+B2	182	-	500	splat quenching and	Singh et al. (2011)
AlCoCrFeNi	SS	NC	BCC	125.1	1138	-	Arc melting	Zhu et al. (2011)
AlCoCrFeNiC$_{0.1}$	SS	NC	BCC+ε	213.2	957	-	Arc melting	Zhu et al. (2011)
AlCoCrFeNiC$_{0.5}$	SS	NC	BCC+ε	180.8	1060	-	Arc melting	Zhu et al. (2011)
AlCoCrFeNiC$_{1.5}$	SS	NC	BCC+ε+Graphite	72.5	1255	-	Arc melting	Zhu et al. (2011)
AlCoCrFeNi	SS	DR	BCC+ Laves	-	1373	520±11	Arc melting	Ma et al. (2002)
AlCoCrFeNb$_{0.25}$Ni	SS	DR+ID	BCC+ Laves	-	1959	668±12	Arc melting	Ma et al. (2002)
AlCoCrFeNb$_{0.5}$Ni	SS	DR+ID	BCC+ Laves	-	2473	747±10	Arc melting	Ma et al. (2002)
AlCoCrCuFe	SS	MNP	FCC+BCC	-	-	770±10	Mechanical alloying	Praveen et al. (2012)
NiCoCrCuFe	SS	MNP	FCC+BCC	-	-	400±10	Mechanical alloying	Praveen et al. (2012)
NiCoCrFe	SS	MNP	FCC+BCC	-	-	490±10	Mechanical alloying	Praveen et al. (2012)
NiCoCuFe	SS	MNP	FCC	-	-	160±10	Mechanical alloying	Praveen et al. (2012)
NiCoFe	SS	MNP	FCC	-	-	230±5	Mechanical alloying	Praveen et al. (2012)

Material	Phase	Morphology	structure	Elastic Modulus (GPa)	Yield Stress (MPa)	Hardness (Hv)	Preparation Method	Ref.
NbTiVTa	SS	DR	BCC	-	1092	-	Arc melting	Yang et al. (2012)
NbTiVTaAl$_{0.5}$	SS	DR	BCC	-	1012	-	Arc melting	Yang et al. (2012)
NbTiVTaAl$_{1.0}$	SS	DR	BCC	-	991	-	Arc melting	Yang et al. (2012)
CoCrFeNi	SS	C	FCC	-	136	140	Arc melting	Shun et al. (2012a)
CoCrFeNiTi$_{0.3}$	SS	DR+ID	FCC+R+σ	-	648	380	Arc melting	Shun et al. (2012a)
CoCrFeNiTi$_{0.5}$	SS	DR+ID	FCC+R+σ+Laves	-	898	515	Arc melting	Shun et al. (2012a)
CoCrFeNiMo$_{0.3}$	SS	DR+ID	FCC+σ	-	305	215	Vacuum arc melting	Shun et al. (2012a)
CoCrFeNiMo$_{0.5}$	SS	DR+ID	FCC+σ	-	510	320	Vacuum arc melting	Shun et al. (2012a)
CoCrFeNiMo$_{0.85}$	SS	DR+ID	FCC +σ+μ	-	929	490	Vacuum arc melting	Shun et al. (2012a)
Al$_{0.2}$CoCrFeNi	SS	CC	FCC	-	-	120	Vacuum arc melting	Wang et al. (2012)
Al$_{0.8}$CoCrFeNi	SS	Side plate	FCC+BCC	-	-	390	Vacuum arc melting	Wang et al. (2012)
Al$_{1.2}$CoCrFeNi	SS	EDR	BCC	-	-	480	Vacuum arc melting	Wang et al. (2012)
Al$_{2.0}$CoCrFeNi	SS	NDR	BCC	-	-	510	Vacuum arc melting	Wang et al. (2012)
FeCoNiCuAlSi	SS	DR+ID	FCC+BCC	-	-	680.4	Copper mold method	Zhuang et al. (2012)
FeCoNiCuAlCr	SS	DR+ID	FCC+BCC	-	-	472	Copper mold method	Zhuang et al. (2012)
FeCoNiCuAlZr	SS+I	-	IM Compound	-	-	472	Copper mold method	Zhuang et al. (2012)
FeCoNiCuAlNd	SS+I	α+β+γ	IM Compound	-	-	577.6	Copper mold method	Zhuang et al. (2012)
Al$_{0.6}$CoNiFeTi$_{0.4}$	SS	P&G	FCC+B2	-	2732	712±12	Spark plasma sintering	Chen et al. (2013)
FeNiCrCo$_{0.3}$Al$_{0.7}$	SS	P&G	FCC+BCC	-	2033±4	624±26	Spark plasma sintering	Chen et al. (2013)
AlCrFeNiMo$_{0.2}$	SS+I	EC	BCC	-	1487.4	548.5	Vacuum arc melting	Dong et al. (2013)
AlCrFeNiMo$_{0.5}$	SS+I	H &LE	BCC	-	1748.6	621.5	Vacuum arc melting	Dong et al. (2013)
AlCrFeNiMo$_{0.8}$	SS+I	H&LE	BCC+σ	-	1512.5	853.8	Vacuum arc melting	Dong et al. (2013)
CoFeNiCrAl$_{0.6}$Ti$_{0.4}$	SS	-	FCC+BCC	-	2080	573	Spark plasma sintering	Fu et al. (2013a)
Co$_{0.5}$FeNiCrTi$_{0.5}$	SS+I	Polygonal bulk	FCC+BCC+σ	-	2650	846	Spark plasma sintering	Fu et al. (2013b)

4. Compression, Tension and Hardness

In this section, the mechanical properties of high entropy alloys are investigated due to their promising properties such as excellent hardness, high resistance to anneal softening, high strength up to 800 ºC, ductility, and good wear resistance (Chen et al., 2005; Tong et al., 2005; Chen et al., 2004). While high entropy alloys have been to some extent investigated at different conditions such as room and elevated temperature and several properties like chemical and thermal properties, mechanical properties of these alloys with solid solution structures have been studied only in more recent years.

Yeh et al. (2004a) have reported the earliest study of mechanical properties of high entropy alloys and presented the effect of aluminum concentration on the hardness of the CuCoNiAl$_x$Fe HEA system. They stated that both binding energy and lattice strains are crucial to strengthening of HEA systems. Hsu et al. (2007) investigated the effect of adding iron (Fe), silver (Ag), and gold (Au) on the hardness of AlCoCrCuNi HEA and found the golden and silver layers of the alloy system have the lowest (104±3) and highest (451±9) hardness, respectively. They mentioned that the reduction of hardness of the Au containing alloy is due to the reduced bonding strength caused by the positive mixing enthalpies of Au with Co and Ni, which lead to the formation of a weaker FCC phase.

Table 2 lists the mechanical properties such as hardness, Young's modulus, and yield strength of HEAs accompanying by their phases, morphology, and structures. Based on the information of Table 2, in Fig. 3(a) and (b) the hardness versus the compositions of high entropy alloys have been plotted for better understanding about the mechanical properties of those. This figure summarizes the compositions of HEA and the Vickers hardness (H_V) (as an engineering property) to compare HEA systems with each other in aspect of the mechanical properties and characterize the different types of microstructures in these kind of alloys. It is found that the hardness and yield strength of the HE alloys composed of the FCC phase are significantly smaller than those of contain the BCC phase. This implies that the BCC phase is much stronger than the FCC phase because of the basic structure factor and solution hardening mechanism. Kao et al. (2009) have studied the hardness of the Al$_x$CoCrFeNi alloys included the FCC, BCC, and FCC-BCC solutions and found the hardness of the alloy increases due to increase in volume fraction of BCC phase (see Fig. 4).
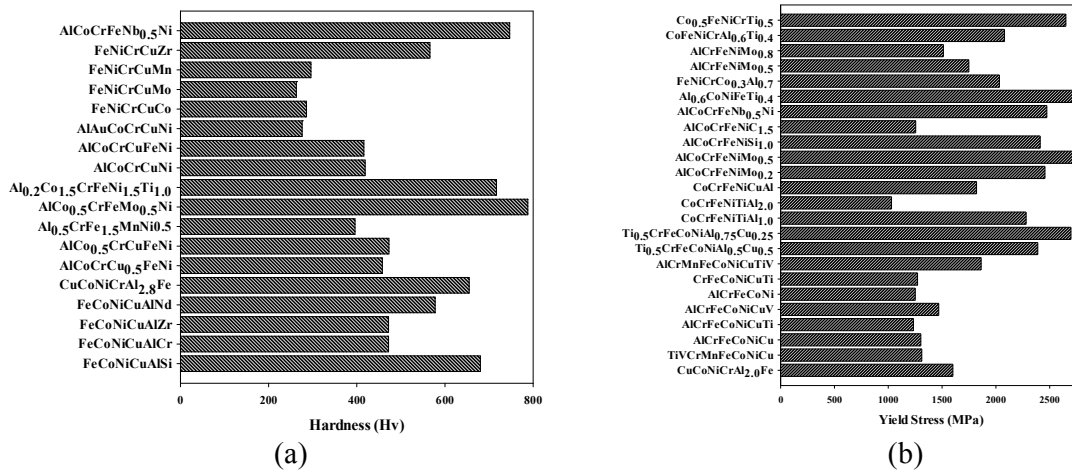
(a)   (b)

Fig. 3. (a) Hardness and (b) yield stress of HEA systems with different compositions

The atomic size difference is also a factor for increasing the lattice distortion and resisting the slip in these alloys (Dieter et al., 1988; Courtney et al., 1990). Zhou et al. (2007b) studied the compressive properties of $Al_x(TiVCrMnFeCoNiCu)_{100-x}$ ($x = 0$, 11.1, 20 and 40 at.%) high-entropy alloys (mentioned in Table 2), and they observed that the compressive strength considerably increased after transforming the solid solution structure from FCC to BCC phase. For example, the compressive strength of $Al_{11.1}(TiVCrMnFeCoNiCu)_{88.9}$ alloy reaches 2.431 GPa. Strain hardening ability has been proposed as an effective factor on the mechanical properties of HEAs by Li et al. (2008) and they mentioned that the reason of the low compressive strength and ultimate strain of AlCrFeCoNiCuTi HE alloy is due to the lack of strain hardening ability on it. Wen et al. (2009) investigated the compressive properties of AlCoCrCuFeNi HEA aged at temperature ranging from 500 to 1000 °C and observed that despite plastic strain, the yield strength of the alloy decreases as the aging temperature increases. Therefore, when the amount of the BCC phases compared to the FCC phases increase, the ductility reduces due to the reduced number of slip systems (Hemphill et al., 2012).Multi-element σ phase is expected to improve hardness and toughness from the practical aspect due to the following reasons, first, the lattice distortion caused by more kinds of solute atoms increases solution hardening, and, second, the reduction of the degree of long-range order lead to enhance toughness (Hsu et al., 2010).Hsu et al. (2010)mentioned that the main factor in determining the hardness of HEAs containing the FCC, BCC, and σ phases is the volume fraction of σ phase in the alloy.
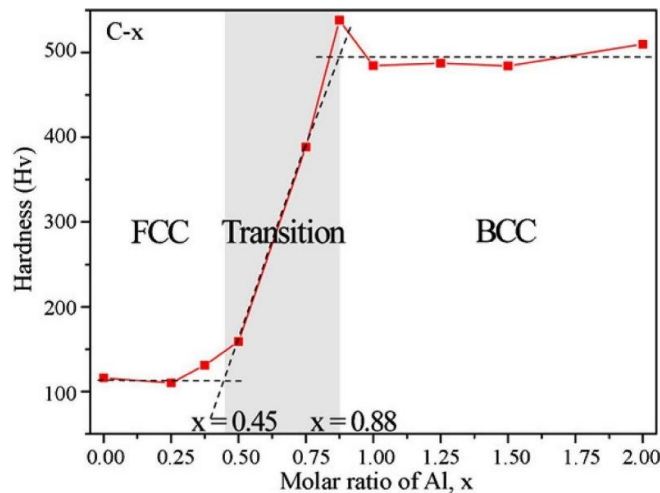

Fig. 4. Hardness of $Al_xCoCrFeNi$ ($0 \leq x \leq 2$) high entropy alloys plot for determining the boundaries of the transition region (Kao et al. 2009).

Some studies have been reported to illustrate the effect of temperature on the mechanical properties of HEAs and understand the relationship among the microstructure, temperature, and the hardness of these alloy systems (Chen et al., 2013; Razuan et al., 2013; Tsai et al., 2011; Chou et al., 2009). Lin and Tsai (2010a) investigated the heat-treated structures of $FeCoNiCrCu_{0.5}$HE alloy at several temperatures with a holding time of 24 h and found that the reduction in the bonding strength between the element atoms caused by thermal behavior associated with the positive mixing enthalpies of several elements and thermal energy declined the hardness of the alloy system (see Fig.5).

Fig. 5.The hardness values of $FeCoNiCrCu_{0.5}$ high-entropy alloy Lin and Tsai (2010a).

Age hardening is the other effective factor on the mechanical properties especially hardness of materials, which usually increases the hardness and strength and decreases the ductility. There are a few studies to present the relation of age hardening and hardness for the HEAs (Lee & Shun, 2013; Shun et al., 2013; Tsao et al., 2012; Ren et al., 2012; Shun & Du, 2009). For example, Shun et al. (2010) studied the age hardening of three FCC structured HEAs, $Al_{0.3}CoCrFeNi$, $Al_{0.3}CoCrFeNiMo_{0.1}$, and $Al_{0.3}CoCrFeNiTi_{0.1}$at 700°C and observed that the hardness increased for 65-89% after 144 h of aging. For further promoting the insight of the mechanical properties and behaviors, one of the interesting works is to study the relationship of the hardness/Young's modulus of high entropy alloys and local atomic structures at different temperatures.

5. Ductility

HEAs often have very attractive mechanical and structural features such as very high strength, reasonable ductility, good work hardening and plasticity, especially at elevated and high temperatures, and these combinations of properties are not seen in conventional alloys. Thus these new kinds of alloys are attracting interests as structural materials for future applications. Lee et al. (2007) have shown the ductility of $Al_{0.5}CoCrCuFeNi$ HE alloy at temperatures up to 800 °C that can have potential applications in high temperature structures and working tools. Some studies investigated the effects of adding element on the ductility of HEA systems (Li et al., 2008; He et al., 2013). Li et al. (2008) indicated the effect of addition of Mn, Ti, and V on the ductility of AlCrFeCoNiCu and found that the AlCrFeCoNiCuV alloy shows a highest strength and largest ductility among them. Based on the

structural factor, one of the most important factor on the ductility of an alloy is the lattice friction during dislocation motion, and lattice friction will be lowered for the structure with more slip system and thus the ductility will increase. Zhang et al. (2010) explained the excellent ductility and large work hardening of the as-annealed CoCrFeNiCuAl HE alloy based on the phase composition, and they found that the FCC structure of the alloy possessed 48 slip system more than that of the BCC structure with 12 slip system and the FCC phases became dominant and therefore the ductility and work hardening effect increased. Zhang et al. (2012c) reported that there surprisingly is no apparent ductile to brittle transition in CoCrFeNiAl HEAs even when the temperatures are lowered from 298 K to 77 K. It is obvious that the ductility of HEAs decrease as the yield stress and compressive strength increase. HEAs with FCC structure usually have good ductility and relatively low strength, but those with BCC structure show much higher strength than FCC typed HE alloys and poor ductility, especially at tension, because the ordering of BCC phase causes the embrittlement of the alloy. The findings in the literature imply that the ductility of the HEAs is very sensitive to the compositions and phases especially FCC and BCC. Therefore, a HEA system with a special mechanical property like ductility can be obtained by appropriately controlling the phases and compositions of that.

6. Fatigue

To investigate the mechanical properties, it is interesting to know more about the mechanism of fatigue damage in high entropy alloys during cyclic deformation. However, there is only one research conducted on the fatigue behavior of HEA system (Hemphill et al., 2012). Recently, Hemphill et al. (2012) have investigated the fatigue behavior of an $Al_{0.5}$CoCrCuFeNi HE alloy and conducted a statistical modeling for the future studies of fatigue characteristics of HEAs. They found that the fatigue behavior of HEAs compares favorably with many conventional alloys such as steels, titanium alloys, and advanced bulk metallic glasses with a fatigue endurance from 540 to 945 MPa. In addition, they have shown that microstructural defects such as aluminum oxide inclusions and microcracks may significantly affect fatigue behavior of HEAs, and the decrease in the number of defects correlates with the increase in fatigue life at various stress levels and thus failure would occur after fewer cycles. On the other hand, they stated that there is not any correlation available between the scatter in the fatigue life and the orientation of loading direction with respect to the different morphologies. Thus the orientation and morphology of the phases do not have any significant influence on the fatigue life.

7. Conclusion

In conclusion, investigations of both microstructure formation and mechanical properties in high entropy alloys as a new brand of metallic materials attract increasingly the researcher's interest to create proportional alloy systems for special applications regarding both optimized properties and cost of production. Two main centerpieces of microstructure formation of high entropy alloys may be found out: 1- fundamental research focuses considerably on the stability and controlling the morphology of these alloys during steady state growth in solidification, 2- the microstructure formation and phases can be predicted based on the two fundamental parameters: first, topological parameters (mainly the atomic size), for example, the atomic size difference for solid solution phases is small against amorphous phases, and second, chemical parameters (the electronegativity, electron concentration or the mixing enthalpy). The fundamental thermodynamic parameters and properties of the elements in preparation of alloys do make a difference on forming the phases such as solid solution, amorphous, and intermetallic phases. It is found that the phases tends to form in the domain defined as follows: 1- solid solution (SS) phases: $0 \leq \delta \leq 8.5$, $-22 \leq \Delta H_{mix} \leq 7$ kJ/mol, and $11 \leq \Delta S_{mix} \leq 19.5$ kJ/mol, 2- the amorphous (AM) phases: $4.5 \leq \delta \leq 18.5$, $-50 \leq \Delta H_{mix} \leq -8$ kJ/mol, and $7 \leq \Delta S_{mix} \leq 17.5$ kJ/mol, and 3- intermetallic (IM) phases: $4 \leq \delta \leq 11.5$, $-35 \leq \Delta H_{mix} \leq -4$ kJ/mol, and $13 \leq \Delta S_{mix} \leq 17.5$ kJ/mol. It is interesting to point out that HEAs generally show a trend of increasing both strength and ductility at different condition as it can be seen in Table 2. While many reasons have been

stated on the suitability of mechanical properties of HEAs in recent years, the relationship between the mechanical properties and atomic structures is still not clear in these alloys and needs to be studied more. This review paper provides valuable study for understanding of the microstructure formation, phase stability, and mechanical properties of high entropy alloys.

References

Cantor, B., & Cahn, R. W. (1976). Metastable alloy phases by co-sputtering. *Acta Metallurgica*, *24*(9), 845-852.

Cantor, B., Chang, I. T. H., Knight, P., & Vincent, A. J. B. (2004). Microstructural development in equiatomic multicomponent alloys. *Materials Science and Engineering: A*, *375*, 213-218.

Chen, M. R., Lin, S. J., Yeh, J. W., Chen, S. K., Huang, Y. S., & Tu, C. P. (2006). Microstructure and Properties of $Al_{0.5}CoCrCuFeNiTi_x$ (x = 0 - 2.0) High-Entropy Alloys.

Chen, S. T., Tang, W. Y., Kuo, Y. F., Chen, S. Y., Tsau, C. H., Shun, T. T., & Yeh, J. W. (2010). Microstructure and properties of age-hardenable $Al_xCrFe_{1.5}MnNi_{0.5}$ alloys. *Materials science & engineering. A, Structural materials: properties, microstructure and processing*, *527*(21-22), 5818-5825.

Chen, T. K., Shun, T. T., Yeh, J. W., & Wong, M. S. (2004). Nanostructured nitride films of multi-element high-entropy alloys by reactive DC sputtering. *Surface and Coatings Technology*, *188*, 193-200.

Chen, W., Fu, Z., Fang, S., Wang, Y., Xiao, H., & Zhu, D. (2013). Processing, microstructure and properties of $Al_{0.6}CoNiFeTi_{0.4}$ high entropy alloy with nanoscale twins. *Materials Science and Engineering: A*, *565*, 439-444.

Chen, Y. L., Hu, Y. H., Tsai, C. W., Hsieh, C. A., Kao, S. W., Yeh, J. W., ... & Chen, S. K. (2009a). Alloying behavior of binary to octonary alloys based on Cu–Ni–Al–Co–Cr–Fe–Ti–Mo during mechanical alloying. *Journal of Alloys and Compounds*, *477*(1), 696-705.

Chen, Y. L., Hu, Y. H., Tsai, C. W., Yeh, J. W., Chen, S. K., & Chang, S. Y. (2009b). Structural evolution during mechanical milling and subsequent annealing of Cu–Ni–Al–Co–Cr–Fe–Ti alloys. *Materials Chemistry and Physics*, *118*(2), 354-361.

Chen, Y. Y., Duval, T., Hung, U. D., Yeh, J. W., & Shih, H. C. (2005). Microstructure and electrochemical properties of high entropy alloys—a comparison with type-304 stainless steel. *Corrosion science*, *47*(9), 2257-2279.

Chou, H. P., Chang, Y. S., Chen, S. K., & Yeh, J. W. (2009). Microstructure, thermophysical and electrical properties in $Al_xCoCrFeNi$ (0≤x≤ 2) high-entropy alloys. *Materials Science and Engineering: B*, *163*(3), 184-189.

Chou, Y. L., Wang, Y. C., Yeh, J. W., & Shih, H. C. (2010a). Pitting corrosion of the high-entropy alloy $Co_{1.5}CrFeNi_{1.5}Ti_{0.5}Mo_{0.1}$ in chloride-containing sulphate solutions. *Corrosion Science*, *52*(10), 3481-3491.

Chou, Y. L., Yeh, J. W., & Shih, H. C. (2010b). The effect of molybdenum on the corrosion behaviour of the high-entropy alloys $Co_{1.5}CrFeNi_{1.5}Ti_{0.5}Mo_x$ in aqueous environments. *Corrosion Science*, *52*(8), 2571-2581.

Chuang, M. H., Tsai, M. H., Wang, W. R., Lin, S. J., & Yeh, J. W. (2011). Microstructure and wear behavior of $Al_xCo_{1.5}CrFeNi_{1.5}Ti_y$ high-entropy alloys. *Acta Materialia*, *59*(16), 6308-6317.

Cohen, M. H., & Turnbull, D. (1961). Composition requirements for glass formation in metallic and ionic systems.

Courtney, T. (1990). Mechanical Behavior of Materials. McGraw-Hill, New York, 173–84.

Dieter, G. E. (1988). Mechanical Metallurgy. SI Metric Editions, McGraw-Hill Book Company, New York 117–21.

Dong, Y., Lu, Y., Kong, J., Zhang, J., & Li, T. (2013). Microstructure and mechanical properties of multi-component $AlCrFeNiMo_x$ high-entropy alloys. *Journal of Alloys and Compounds*, *573*, 96-101.

Egami, T., & Waseda, Y. (1984). Atomic size effect on the formability of metallic glasses. *Journal of non-crystalline solids*, *64*(1), 113-134.

Fu, Z., Chen, W., Fang, S., Zhang, D., Xiao, H., & Zhu, D. (2013a). Alloying behavior and deformation twinning in a CoNiFeCrAl$_{0.6}$Ti$_{0.4}$ high entropy alloy processed by spark plasma sintering. *Journal of Alloys and Compounds*, *553*, 316-323.

Fu, Z., Chen, W., Xiao, H., Zhou, L., Zhu, D., & Yang, S. (2013b). Fabrication and properties of nanocrystalline Co$_{0.5}$FeNiCrTi$_{0.5}$ high entropy alloy by MA–SPS technique. *Materials & Design*, *44*, 535-539.

Gao, X. Q., Zhao, K., Ke, H. B., Ding, D. W., Wang, W. H., & Bai, H. Y. (2011). High mixing entropy bulk metallic glasses. *Journal of Non-Crystalline Solids*, *357*(21), 3557-3560.

Guo, S., Ng, C., & Liu, C. T. (2013). Anomalous solidification microstructures in Co-free Al$_x$CrCuFeNi$_2$ high-entropy alloys. *Journal of Alloys and Compounds*, *557*, 77-81.

He, J. Y., Liu, W. H., Wang, H., Wu, Y., Liu, X. J., Nieh, T. G., & Lu, Z. P. (2014). Effects of Al addition on structural evolution and tensile properties of the FeCoNiCrMn high-entropy alloy system. *Acta Materialia*, *62*, 105-113.

Hemphill, M. A., Yuan, T., Wang, G. Y., Yeh, J. W., Tsai, C. W., Chuang, A., & Liaw, P. K. (2012). Fatigue behavior of Al$_{0.5}$CoCrCuFeNi high entropy alloys. *Acta Materialia*, *60*(16), 5723-5734.

Hsieh, K. C., Yu, C. F., Hsieh, W. T., Chiang, W. R., Ku, J. S., Lai, J. H., ... & Yang, C. C. (2009). The microstructure and phase equilibrium of new high performance high-entropy alloys. *Journal of Alloys and Compounds*, *483*(1), 209-212.

Hsu, C. Y., Juan, C. C., Wang, W. R., Sheu, T. S., Yeh, J. W., & Chen, S. K. (2011). On the superior hot hardness and softening resistance of AlCoCr$_x$FeMo$_{0.5}$Ni high-entropy alloys. *Materials Science and Engineering: A*, *528*(10), 3581-3588.

Hsu, C. Y., Wang, W. R., Tang, W. Y., Chen, S. K., & Yeh, J. W. (2010). Microstructure and Mechanical Properties of New AlCo$_x$CrFeMo$_{0.5}$Ni High-Entropy Alloys. *Advanced Engineering Materials*, *12*(1-2), 44-49.

Hsu, U. S., Hung, U. D., Yeh, J. W., Chen, S. K., Huang, Y. S., & Yang, C. C. (2007). Alloying behavior of iron, gold and silver in AlCoCrCuNi-based equimolar high-entropy alloys. *Materials Science and Engineering: A*, *460*, 403-408.

Huang, Y. S., Chen, L., Lui, H. W., Cai, M. H., & Yeh, J. W. (2007). Microstructure, hardness, resistivity and thermal stability of sputtered oxide films of AlCoCrCu$_{0.5}$NiFe high-entropy alloy. *Materials Science and Engineering: A*,*457*(1), 77-83.

Inoue, A. (2000). Stabilization of metallic supercooled liquid and bulk amorphous alloys. *Acta materialia*, *48*(1), 279-306.

Kao, Y. F., Chen, T. J., Chen, S. K., & Yeh, J. W. (2009). Microstructure and mechanical property of as-cast,-homogenized, and-deformed Al$_x$CoCrFeNi ($0 \leq x \leq 2$) high-entropy alloys. *Journal of Alloys and Compounds*,*488*(1), 57-64.

Kaufman, L., &Bernstein, H,. (1970). Computer Calculation of Phase Diagrams New York: Academic Press.

Ke, G. Y., Chen, S. K., Hsu, T., & Yeh, J. W. (2006). FCC and BCC equivalents in as-cast solid solutions of Al$_x$Co$_y$Cr$_z$Cu$_{0.5}$FeVNiW high-entropy alloys. In *Annales de chimie* (Vol. 31, No. 6, pp. 669-683). Lavoisier.

Khalifa, W., Samuel, F. H., & Gruzleski, J. E. (2003). Iron intermetallic phases in the Al corner of the Al-Si-Fe system. *Metallurgical and Materials Transactions A*,*34*(3), 807-825.

Koundinya, N. T. B. N., Babu, C. S., Sivaprasad, K., Susila, P., Babu, N. K., & Baburao, J. (2013). Phase Evolution and Thermal Analysis of Nanocrystalline AlCrCuFeNiZn High Entropy Alloy Produced by Mechanical Alloying. *Journal of materials engineering and performance*, *22*(10), 3077-3084.

Lee, C. F., & Shun, T. T. (2014). Age Hardening of the Al$_{0.5}$CoCrNiTi$_{0.5}$ High-Entropy Alloy. *Metallurgical and Materials Transactions A*, *45*(1), 191-195.

Lee, C. P., Chen, Y. Y., Hsu, C. Y., Yeh, J. W., & Shih, H. C. (2007). The Effect of Boron on the Corrosion Resistance of the High Entropy Alloys $Al_{0.5}CoCrCuFeNiB_x$. *Journal of the Electrochemical Society*, *154*(8), C424-C430.

Li, A., Ma, D., & Zheng, Q. (2014). Effect of Cr on Microstructure and Properties of a Series of $AlTiCr_xFeCoNiCu$ High-Entropy Alloys. *Journal of materials engineering and performance*, *23*(4), 1197-1203.

Li, B. S., Wang, Y. P., Ren, M. X., Yang, C., & Fu, H. Z. (2008). Effects of Mn, Ti and V on the microstructure and properties of AlCrFeCoNiCu high entropy alloy. *Materials Science and Engineering: A*, *498*(1), 482-486.

Li, C., Li, J. C., Zhao, M., & Jiang, Q. (2009). Effect of alloying elements on microstructure and properties of multiprincipal elements high-entropy alloys. *Journal of Alloys and Compounds*, *475*(1), 752-757.

Li, C., Li, J. C., Zhao, M., & Jiang, Q. (2010). Effect of aluminum contents on microstructure and properties of $Al_xCoCrFeNi$ alloys. *Journal of Alloys and Compounds*, *504*, S515-S518.

Li, Y., Poon, S. J., Shiflet, G. J., Xu, J., Kim, D. H., & Löffler, J. F. (2007). Formation of bulk metallic glasses and their composites. *MRS bulletin*, *32*(08), 624-628.

Lin, C. M., & Tsai, H. L. (2010a). Equilibrium phase of high-entropy $FeCoNiCrCu_{0.5}$ alloy at elevated temperature. *Journal of Alloys and Compounds*,*489*(1), 30-35.

Lin, C. M., & Tsai, H. L. (2011). Evolution of microstructure, hardness, and corrosion properties of high-entropy $Al_{0.5}CoCrFeNi$ alloy. *Intermetallics*,*19*(3), 288-294.

Lin, C. M., Tsai, H. L., & Bor, H. Y. (2010b). Effect of aging treatment on microstructure and properties of high-entropy $Cu_{0.5}CoCrFeNi$ alloy. *Intermetallics*, *18*(6), 1244-1250.

Lin, M. I., Tsai, M. H., Shen, W. J., & Yeh, J. W. (2010c). Evolution of structure and properties of multi-component $(AlCrTaTiZr)O_x$ films. *Thin Solid Films*, *518*(10), 2732-2737.

Lin, Y. C., & Cho, Y. H. (2009). Elucidating the microstructural and tribological characteristics of NiCrAlCoCu and NiCrAlCoMo multicomponent alloy clad layers synthesized in situ. *Surface and Coatings Technology*, *203*(12), 1694-1701.

Liu, L., Zhu, J. B., Li, J. C., & Jiang, Q. (2012). Microstructure and Magnetic Properties of $FeNiCuMnTiSn_x$ High Entropy Alloys. *Advanced Engineering Materials*, *14*(10), 919-922.

Ma, L., Wang, L., Zhang, T., & Inoue, A. (2002). Bulk glass formation of Ti-Zr-Hf-Cu-M (M= Fe, Co, Ni) alloys. *Materials Transactions*, *43*(2), 277-280.

Ma, S. G., & Zhang, Y. (2012). Effect of Nb addition on the microstructure and properties of AlCoCrFeNi high-entropy alloy. *Materials Science and Engineering: A*, *532*, 480-486.

Manzoni, A., Daoud, H., Mondal, S., van Smaalen, S., Völkl, R., Glatzel, U., & Wanderka, N. (2013a). Investigation of phases in $Al_{23}Co_{15}Cr_{23}Cu_8Fe_{15}Ni_{16}$ and $Al_8Co_{17}Cr_{17}Cu_8Fe_{17}Ni_{33}$ high entropy alloys and comparison with equilibrium phases predicted by Thermo-Calc. *Journal of Alloys and Compounds*,*552*(Complete), 430-436.

Manzoni, A., Daoud, H., Völkl, R., Glatzel, U., & Wanderka, N. (2013b). Phase separation in equiatomic AlCoCrFeNi high-entropy alloy. *Ultramicroscopy*, *132*, 212-215.

Mridha, S., Samal, S., Khan, P. Y., & Biswas, K. (2013). Processing and Consolidation of Nanocrystalline Cu-Zn-Ti-Fe-Cr High-Entropy Alloys via Mechanical Alloying. *Metallurgical and Materials Transactions A*, *44*(10), 4532-4541.

Ng, C., Guo, S., Luan, J., Shi, S., & Liu, C. T. (2012). Entropy-driven phase stability and slow diffusion kinetics in an $Al_{0.5}CoCrCuFeNi$ high entropy alloy. *Intermetallics*, *31*, 165-172.

Otto, F., Dlouhý, A., Somsen, C., Bei, H., Eggeler, G., & George, E. P. (2013a). The influences of temperature and microstructure on the tensile properties of a CoCrFeMnNi high-entropy alloy. *Acta Materialia*, *61*(15), 5743-5755.

Otto, F., Yang, Y., Bei, H., & George, E. P. (2013b). Relative effects of enthalpy and entropy on the phase stability of equiatomic high-entropy alloys. *Acta Materialia*,*61*(7), 2628-2638.

Perricone, M. J., DuPont, J. N., & Cieslak, M. J. (2003). Solidification of hastelloy alloys: an alternative interpretation. *Metallurgical and Materials Transactions A*,*34*(5), 1127-1132.

Praveen, S., Anupam, A., Sirasani, T., Murty, B. S., & Kottada, R. S. (2013). Characterization of Oxide Dispersed AlCoCrFe High Entropy Alloy Synthesized by Mechanical Alloying and Spark Plasma Sintering. *Transactions of the Indian Institute of Metals*, *66*(4), 369-373.

Praveen, S., Murty, B. S., & Kottada, R. S. (2012). Alloying behavior in multi-component AlCoCrCuFe and NiCoCrCuFe high entropy alloys. *Materials Science and Engineering: A*, *534*, 83-89.

Qiu, X. W., & Liu, C. G. (2013). Microstructure and properties of $Al_2CrFeCoCuTiNi_x$ high-entropy alloys prepared by laser cladding. *Journal of Alloys and Compounds*, *553*, 216-220.

R.A. Swalin, E. Burke, B. Chalmers, &AlKrumhansl J. (1991) Thermodynamics of Solids. second ed, JohnWiley & Sons, New York, NY.

Ranganathan, S. (2003). Alloyed pleasures: Multimetallic cocktails. *Current Science*, *85*(5), 1404-1406.

Razuan, R., Jani, N. A., Harun, M. K., & Talari, M. K. (2013). Microstructure and Hardness Properties Investigation of Ti and Nb Added $FeNiAlCuCrTi_xNb_y$ High Entropy Alloys. *Transactions of the Indian Institute of Metals*, *66*(4), 309-312.

Ren, B., Liu, Z. X., Cai, B., Wang, M. X., & Shi, L. (2012). Aging behavior of a $CuCr_2Fe_2NiMn$ high-entropy alloy. *Materials & Design*, *33*, 121-126.

Senkov, O. N., & Woodward, C. F. (2011a). Microstructure and properties of a refractory $NbCrMo_{0.5}Ta_{0.5}TiZr$ alloy. *Materials Science and Engineering: A*, *529*, 311-320.

Senkov, O. N., Wilks, G. B., Miracle, D. B., Chuang, C. P., & Liaw, P. K. (2010). Refractory high-entropy alloys. *Intermetallics*, *18*(9), 1758-1765.

Senkov, O. N., Wilks, G. B., Scott, J. M., & Miracle, D. B. (2011b). Mechanical properties of $Nb_{25}Mo_{25}Ta_{25}W_{25}$ and $V_{20}Nb_{20}Mo_{20}Ta_{20}W_{20}$ refractory high entropy alloys. *Intermetallics*, *19*(5), 698-706.

Sheng, H. F., M. Gong, and L. M. Peng. "Microstructural characterization and mechanical properties of an $Al_{0.5}CoCrFeCuNi$ high-entropy alloy in as-cast and heat-treated/quenched conditions." *Materials Science and Engineering: A* 567 (2013): 14-20.

Shun, T. T., & Du, Y. C. (2009). Age hardening of the $Al_{0.3}CoCrFeNiC_{0.1}$ high entropy alloy. *Journal of alloys and compounds*, *478*(1-2), 269-272.

Shun, T. T., Chang, L. Y., & Shiu, M. H. (2012a). Microstructure and mechanical properties of multiprincipal component $CoCrFeNiMo_x$ alloys.*Materials Characterization*, *70*, 63-67.

Shun, T. T., Chang, L. Y., & Shiu, M. H. (2012b). Microstructures and mechanical properties of multiprincipal component $CoCrFeNiTi_x$ alloys. *Materials Science and Engineering: A*, *556*, 170-174.

Shun, T. T., Chang, L. Y., & Shiu, M. H. (2013). Age-hardening of the $CoCrFeNiMo_{0.85}$ high-entropy alloy. *Materials Characterization*, *81*, 92-96.

Shun, T. T., Hung, C. H., & Lee, C. F. (2010). The effects of secondary elemental Mo or Ti addition in $Al_{0.3}CoCrFeNi$ high-entropy alloy on age hardening at 700° C. *Journal of Alloys and Compounds*, *495*(1), 55-58.

Singh, S., Wanderka, N., Murty, B. S., Glatzel, U., & Banhart, J. (2011). Decomposition in multi-component AlCoCrCuFeNi high-entropy alloy. *Acta Materialia*, *59*(1), 182-190.

Sriharitha, R., Murty, B. S., & Kottada, R. S. (2013). Phase formation in mechanically alloyed $Al_xCoCrCuFeNi$ (x= 0.45, 1, 2.5, 5 mol) high entropy alloys. *Intermetallics*, *32*, 119-126.

Takeuchi, A., & Inoue, A. (2000). Calculations of mixing enthalpy and mismatch entropy for ternary amorphous alloys. *Materials Transactions-JIM*, *41*(11), 1372-1378.

Takeuchi, A., & Inoue, A. (2001). Quantitative evaluation of critical cooling rate for metallic glasses. *Materials Science and Engineering: A*, *304*, 446-451.

Tariq, N. H., Naeem, M., Hasan, B. A., Akhter, J. I., & Siddique, M. (2013). Effect of W and Zr on structural, thermal and magnetic properties of AlCoCrCuFeNi high entropy alloy. *Journal of Alloys and Compounds*, *556*, 79-85.

Tong, C. J., Chen, Y. L., Yeh, J. W., Lin, S. J., Chen, S. K., Shun, T. T., ... & Chang, S. Y. (2005). Microstructure characterization of Al_xCoCrCuFeNi high-entropy alloy system with multiprincipal elements. *Metallurgical and Materials Transactions A*,*36*(4), 881-893.

Tsai, C. W., Chen, Y. L., Tsai, M. H., Yeh, J. W., Shun, T. T., & Chen, S. K. (2009). Deformation and annealing behaviors of high-entropy alloy $Al_{0.5}$CoCrCuFeNi. *Journal of Alloys and Compounds*, *486*(1), 427-435.

Tsai, D. C., Chang, Z. C., Kuo, B. H., Shiao, M. H., Chang, S. Y., & Shieu, F. S. (2013a). Structural morphology and characterization of (AlCrMoTaTi) N coating deposited via magnetron sputtering. *Applied Surface Science*, *282*, 789-797.

Tsai, K. Y., Tsai, M. H., & Yeh, J. W. (2013b). Sluggish diffusion in Co–Cr–Fe–Mn–Ni high-entropy alloys. *Acta Materialia*, *61*(13), 4887-4897.

Tsai, M. H., Wang, C. W., Tsai, C. W., Shen, W. J., Yeh, J. W., Gan, J. Y., & Wu, W. W. (2011). Thermal stability and performance of NbSiTaTiZr high-entropy alloy barrier for copper metallization. *Journal of the Electrochemical Society*, *158*(11), H1161-H1165.

Tsai, M. H., Yuan, H., Cheng, G., Xu, W., Jian, W. W., Chuang, M. H., ... & Zhu, Y. (2013c). Significant hardening due to the formation of a sigma phase matrix in a high entropy alloy. *Intermetallics*, *33*, 81-86.

Tsai, M. H., Yuan, H., Cheng, G., Xu, W., Tsai, K. Y., Tsai, C. W., ... & Zhu, Y. T. (2013d). Morphology, structure and composition of precipitates in $Al_{0.3}$CoCrCu$_{0.5}$FeNi high-entropy alloy. *Intermetallics*, *32*, 329-336.

Tsao, L. C., Chen, C. S., & Chu, C. P. (2012). Age hardening reaction of the $Al_{0.3}$CrFe$_{1.5}$MnNi$_{0.5}$ high entropy alloy.*Materials & Design*, *36*, 854-858.

Tung, C. C., Yeh, J. W., Shun, T. T., Chen, S. K., Huang, Y. S., & Chen, H. C. (2007). On the elemental effect of AlCoCrCuFeNi high-entropy alloy system. *Materials letters*, *61*(1), 1-5.

Varalakshmi, S., Kamaraj, M., & Murty, B. S. (2008). Synthesis and characterization of nanocrystalline AlFeTiCrZnCu high entropy solid solution by mechanical alloying. *Journal of Alloys and Compounds*, *460*(1), 253-257.

Wang, F. J., Zhang, Y., & Chen, G. L. (2009a). Atomic packing efficiency and phase transition in a high entropy alloy. *Journal of Alloys and Compounds*, *478*(1), 321-324.

Wang, W. R., Wang, W. L., Wang, S. C., Tsai, Y. C., Lai, C. H., & Yeh, J. W. (2012). Effects of Al addition on the microstructure and mechanical property of Al_xCoCrFeNi high-entropy alloys. *Intermetallics*, *26*, 44-51.

Wang, X. F., Zhang, Y., Qiao, Y., & Chen, G. L. (2007). Novel microstructure and properties of multicomponent CoCrCuFeNiTi$_x$ alloys. *Intermetallics*, *15*(3), 357-362.

Wang, Y. P., Li, B. S., & Fu, H. Z. (2009b). Solid Solution or Intermetallics in a High-Entropy Alloy. *Advanced Engineering Materials*, *11*(8), 641-644.

Wang, Y. P., Li, B. S., Ren, M. X., Yang, C., & Fu, H. Z. (2008). Microstructure and compressive properties of AlCrFeCoNi high entropy alloy. *Materials Science and Engineering: A*, *491*(1), 154-158.

Wang, Y. P., Li, D. Y., Parent, L., & Tian, H. (2011). Improving the wear resistance of white cast iron using a new concept–High-entropy microstructure. *Wear*, *271*(9), 1623-1628.

Wang, Y. P., Li, D. Y., Parent, L., & Tian, H. (2013). Performances of hybrid high-entropy high-Cr cast irons during sliding wear and air-jet solid-particle erosion. *Wear*, *301*(1), 390-397.

Wen, L. H., Kou, H. C., Li, J. S., Chang, H., Xue, X. Y., & Zhou, L. (2009). Effect of aging temperature on microstructure and properties of AlCoCrCuFeNi high-entropy alloy. *Intermetallics*, *17*(4), 266-269.

Wu, J. M., Lin, S. J., Yeh, J. W., Chen, S. K., Huang, Y. S., & Chen, H. C. (2006). Adhesive wear behavior of Al_xCoCrCuFeNi high-entropy alloys as a function of aluminum content. *Wear*, *261*(5), 513-519.

Yang, X., Zhang, Y., & Liaw, P. K. (2012). Microstructure and compressive properties of NbTiVTaAl$_x$ high entropy alloys. *Procedia Engineering*, *36*, 292-298.

Yeh, J. W. (2013). Alloy design strategies and future trends in high-entropy alloys. *JOM*, *65*(12), 1759-1771.

Yeh, J. W., Chang, S. Y., Hong, Y. D., Chen, S. K., & Lin, S. J. (2007). Anomalous decrease in X-ray diffraction intensities of Cu–Ni–Al–Co–Cr–Fe–Si alloy systems with multi-principal elements. *Materials chemistry and physics*, *103*(1), 41-46.

Yeh, J. W., Chen, S. K., Lin, S. J., Gan, J. Y., Chin, T. S., Shun, T. T., ... & Chang, S. Y. (2004a). Nanostructured High-Entropy Alloys with Multiple Principal Elements: Novel Alloy Design Concepts and Outcomes. *Advanced Engineering Materials*, *6*(5), 299-303.

Yeh, J. W., Lin, S. J., Chin, T. S., Gan, J. Y., Chen, S. K., Shun, T. T., ... & Chou, S. Y. (2004b). Formation of simple crystal structures in Cu-Co-Ni-Cr-Al-Fe-Ti-V alloys with multiprincipal metallic elements. *Metallurgical and Materials Transactions A*, *35*(8), 2533-2536.

Yu, Y., Liu, W. M., Zhang, T. B., Li, J. S., Wang, J., Kou, H. C., & Li, J. (2014). Microstructure and Tribological Properties of $AlCoCrFeNiTi_{0.5}$ High-Entropy Alloy in Hydrogen Peroxide Solution. *Metallurgical and Materials Transactions A*, *45*(1), 201-207.

Zhang, C., Zhang, F., Chen, S., & Cao, W. (2012a). Computational thermodynamics aided high-entropy alloy design. *JOM*, *64*(7), 839-845.

Zhang, H., He, Y. Z., Pan, Y., & Pei, L. Z. (2011). Phase selection, microstructure and properties of laser rapidly solidified $FeCoNiCrAl_2Si$ coating. *Intermetallics*, *19*(8), 1130-1135.

Zhang, H., He, Y., & Pan, Y. (2013). Enhanced hardness and fracture toughness of the laser-solidified $FeCoNiCrCuTiMoAlSiB_{0.5}$ high-entropy alloy by martensite strengthening. *Scripta Materialia*, *69*(4), 342-345.

Zhang, K. B., Fu, Z. Y., Zhang, J. Y., Shi, J., Wang, W. M., Wang, H., ... & Zhang, Q. J. (2010). Annealing on the structure and properties evolution of the CoCrFeNiCuAl high-entropy alloy. *Journal of Alloys and Compounds*, *502*(2), 295-299.

Zhang, K. B., Fu, Z. Y., Zhang, J. Y., Wang, W. M., Wang, H., Wang, Y. C., ... & Shi, J. (2009). Microstructure and mechanical properties of $CoCrFeNiTiAl_x$ high-entropy alloys. *Materials Science and Engineering: A*, *508*(1), 214-219.

Zhang, Y., Ma, S. G., & Qiao, J. W. (2012b). Morphology transition from dendrites to equiaxed grains for AlCoCrFeNi high-entropy alloys by copper mold casting and Bridgman solidification. *Metallurgical and Materials Transactions A*, *43*(8), 2625-2630.

Zhang, Y., Yang, X., & Liaw, P. K. (2012c). Alloy design and properties optimization of high-entropy alloys. *JOM*, *64*(7), 830-838.

Zhang, Y., Zhou, Y. J., Lin, J. P., Chen, G. L., & Liaw, P. K. (2008). Solid-Solution Phase Formation Rules for Multi-component Alloys. *Advanced Engineering Materials*, *10*(6), 534-538.

Zhou, Y. J., Zhang, Y., Wang, Y. L., & Chen, G. L. (2007a). Microstructure and compressive properties of multicomponent $Al_x(TiVCrMnFeCoNiCu)_{(100-x)}$ high-entropy alloys. *Materials Science and Engineering: A*, *454*, 260-265.

Zhou, Y. J., Zhang, Y., Wang, Y. L., & Chen, G. L. (2007b). Solid solution alloys of $AlCoCrFeNiTi_x$ with excellent room-temperature mechanical properties. *Applied physics letters*, *90*(18), 181904-181904.

Zhu, J. M., Fu, H. M., Zhang, H. F., Wang, A. M., Li, H., & Hu, Z. Q. (2010a). Microstructures and compressive properties of multicomponent $AlCoCrFeNiMo_x$ alloys. *Materials Science and Engineering: A*, *527*(26), 6975-6979.

Zhu, J. M., Fu, H. M., Zhang, H. F., Wang, A. M., Li, H., & Hu, Z. Q. (2010b). Synthesis and properties of multiprincipal component $AlCoCrFeNiSi_x$ alloys. *Materials Science and Engineering: A*, *527*(27), 7210-7214.

Zhu, J. M., Fu, H. M., Zhang, H. F., Wang, A. M., Li, H., & Hu, Z. Q. (2011). Microstructure and compressive properties of multiprincipal component $AlCoCrFeNiC_x$ alloys. *Journal of Alloys and Compounds*, *509*(8), 3476-3480.

Zhuang, Y. X., Liu, W. J., Chen, Z. Y., Xue, H. D., & He, J. C. (2012). Effect of elemental interaction on microstructure and mechanical properties of FeCoNiCuAl alloys. *Materials Science and Engineering: A*, *556*, 395-399.